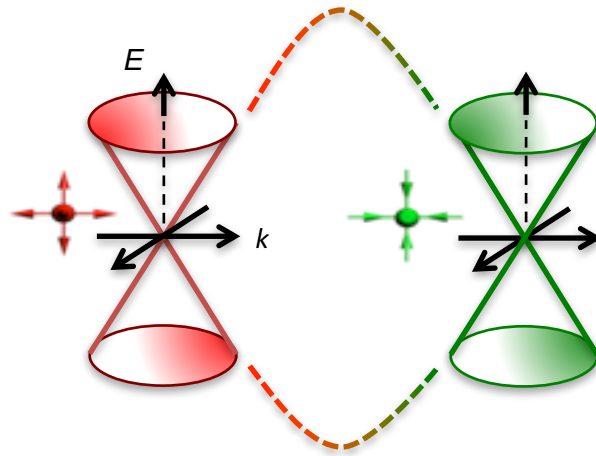


# Berry curvature dipole in Weyl materials



**Binghai Yan**

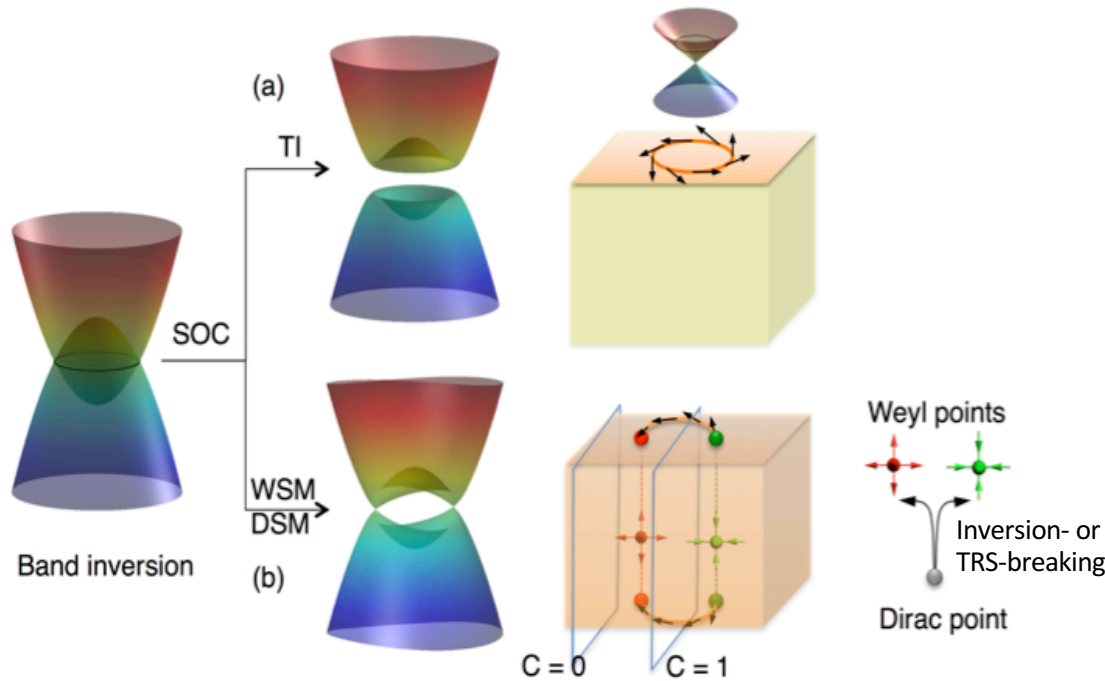
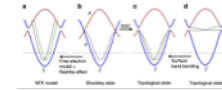
Weizmann Institute of Science, Israel

[www.weizmann.ac.il/condmat/Yan/](http://www.weizmann.ac.il/condmat/Yan/)



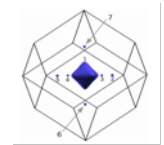
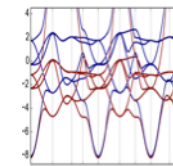
*arXiv:1708.08589.*

# Topological insulators and topological metals



Topological surface states on Gold (111)  
Yan 15'

Figure from Annu. Rev. Condens. Matter Phys. 8, 337-354 (2017)



Weyl points in *bcc* Fe  
Vanderbilt 15'

More commonly existing in materials than thought.

# Weyl SemiMetal (WSM)

$$\left( \beta mc^2 + c \left( \sum_{n=1}^3 \alpha_n p_n \right) \right) \psi(x,t) = i\hbar \frac{\partial \psi(x,t)}{\partial t}$$

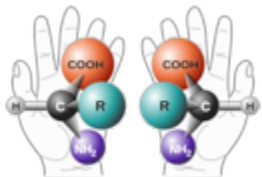
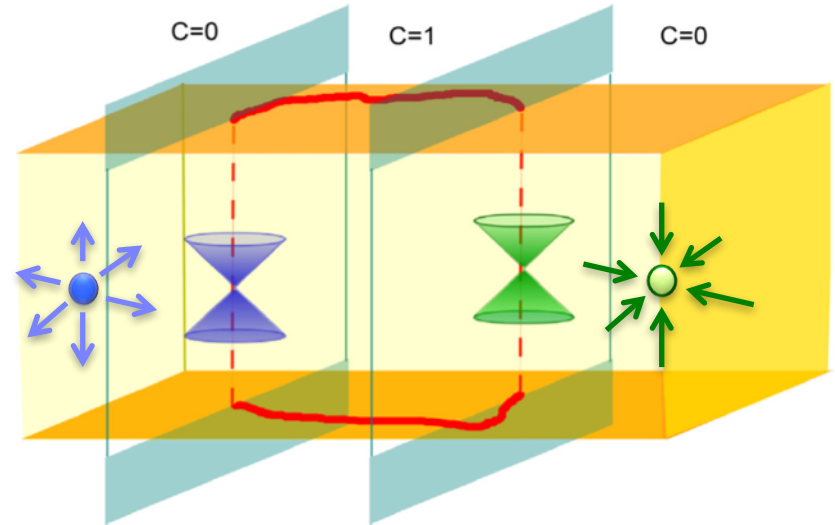
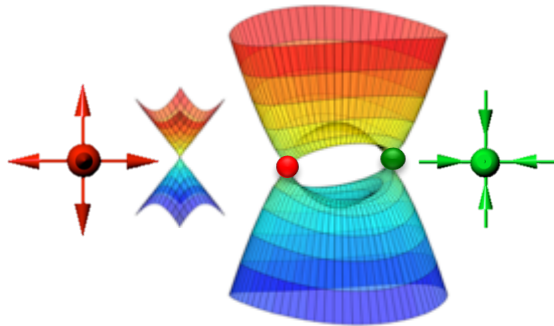
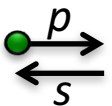
$$m = 0$$

$$i \frac{\partial \psi}{\partial t} = \pm c \vec{p} \cdot \vec{\sigma} \psi$$



Hermann Weyl  
1929'

$$H = \pm \sigma \cdot p$$

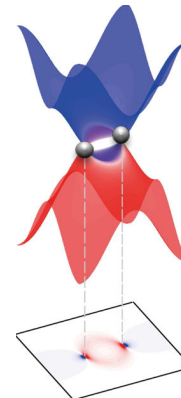
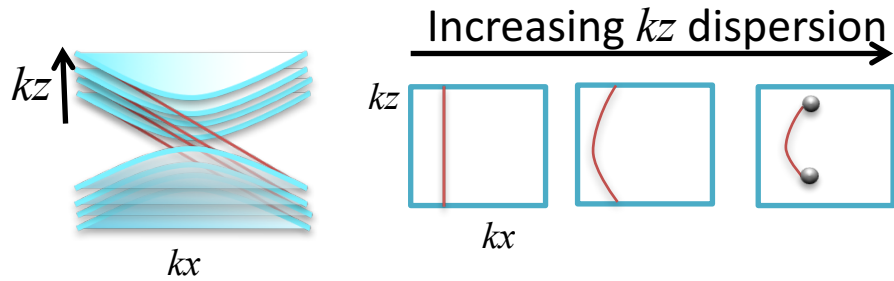
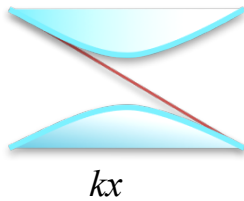
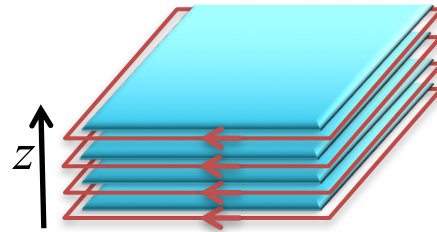
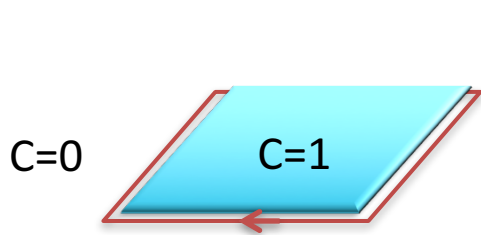


X. Wan et al PRB 83, 205101 (2011).

S. Murakami, New Journal of Physics 10, 029802 (2008).

G. E. Volovik, *The Universe in A Helium Droplet* (Clarendon Press, Oxford, 2003).

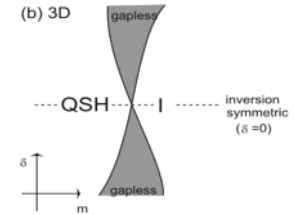
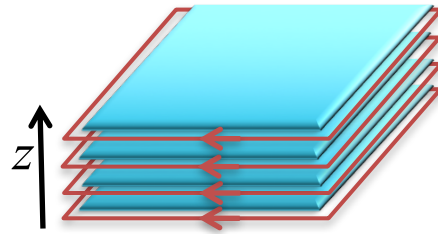
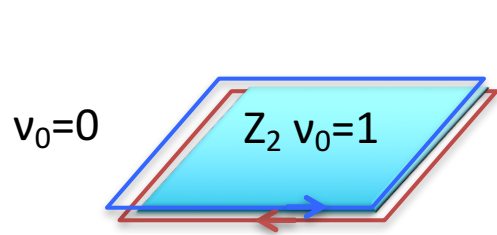
# Quantum Hall effect or Chern insulator



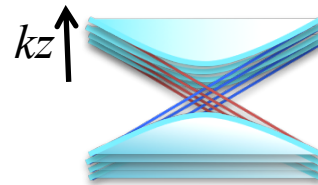
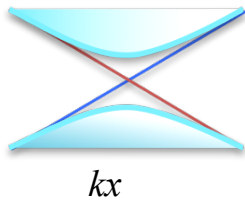
$$AHE = \frac{k_z}{\pi} G_0$$

$$SHE = \frac{k_z}{\pi} G_0 \frac{\hbar}{2e}$$

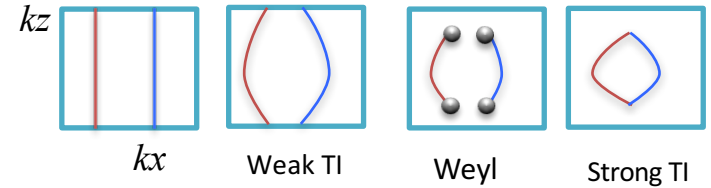
# Topological Insulator



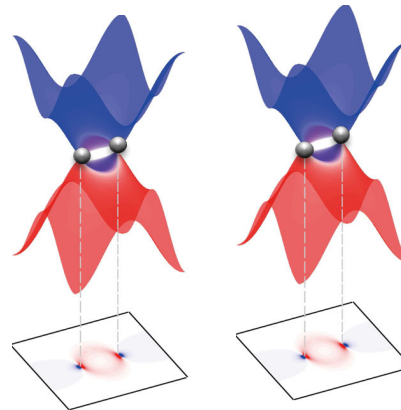
Murakami 2008'.



Increasing  $kz$  dispersion  $\rightarrow$



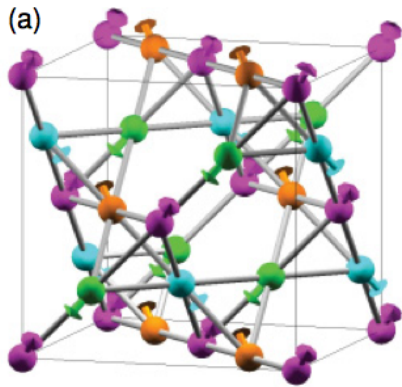
Time-Reversal Symmetry (TRS)



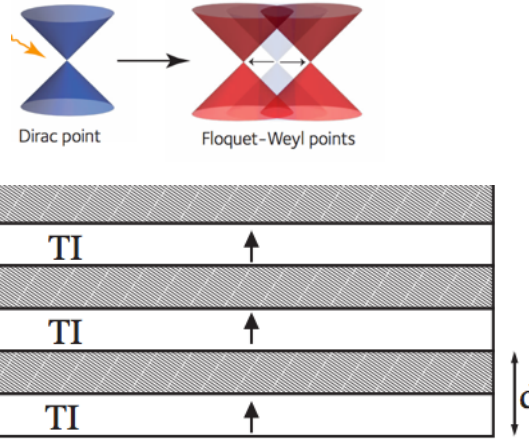
$$AHE = 0$$

$$SHE = \frac{k_z}{\pi} G_0 \frac{\hbar}{2e} \times 2$$

# WSM materials

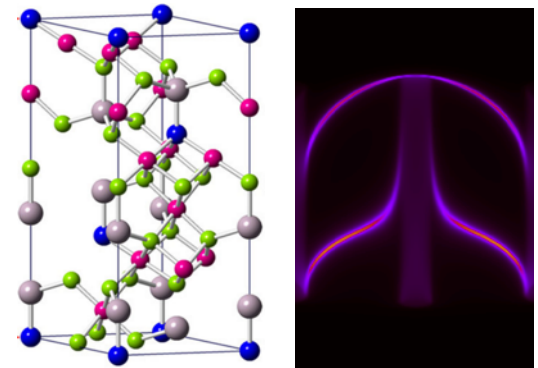


Pyrochlore  $Y_2Ir_2O_7$   
(noncollinear AFM)  
X. Wan, et al.  
PRB **83**, 205101 (2011).



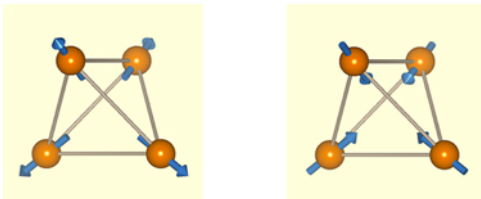
Super lattice: TI + FM

A. Burkov and L. Balents,  
PRL **107**, 127205 (2011).



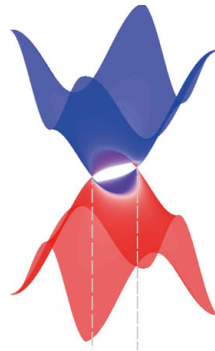
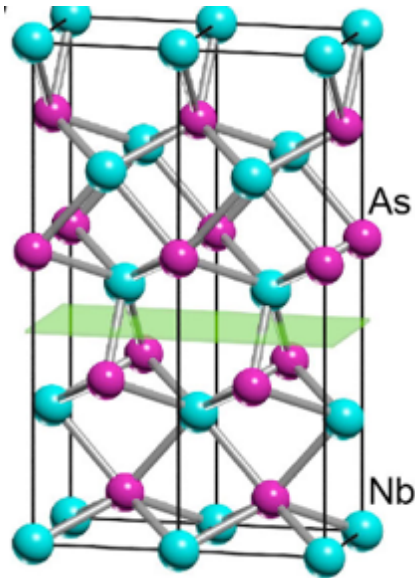
$HgCr_2Se_4$  (FM)

G. Xu et al.  
PRL **107**, 186806 (2011).



Physically interesting,  
Chemically more interesting!

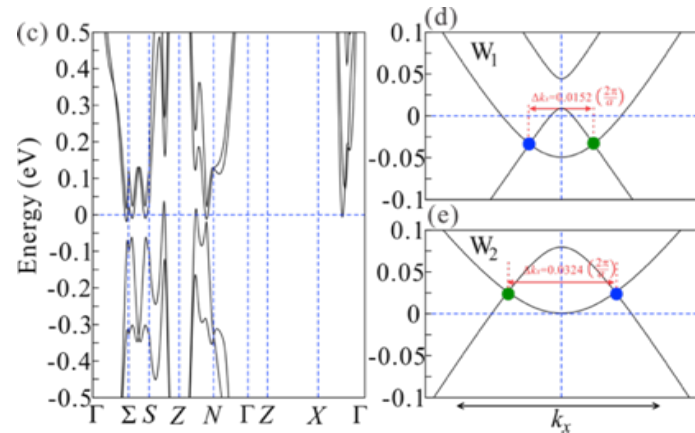
# WSM materials



Dream



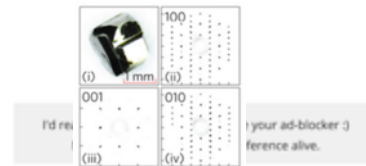
Reality



TaAs, TaP, NbAs, NbP

H.M. Weng *et al.* *Phys. Rev. X* **5**, 011029 (2015).  
 S. M. Huang *et al.* *Nature Commun.* **6**, 7373 (2015).

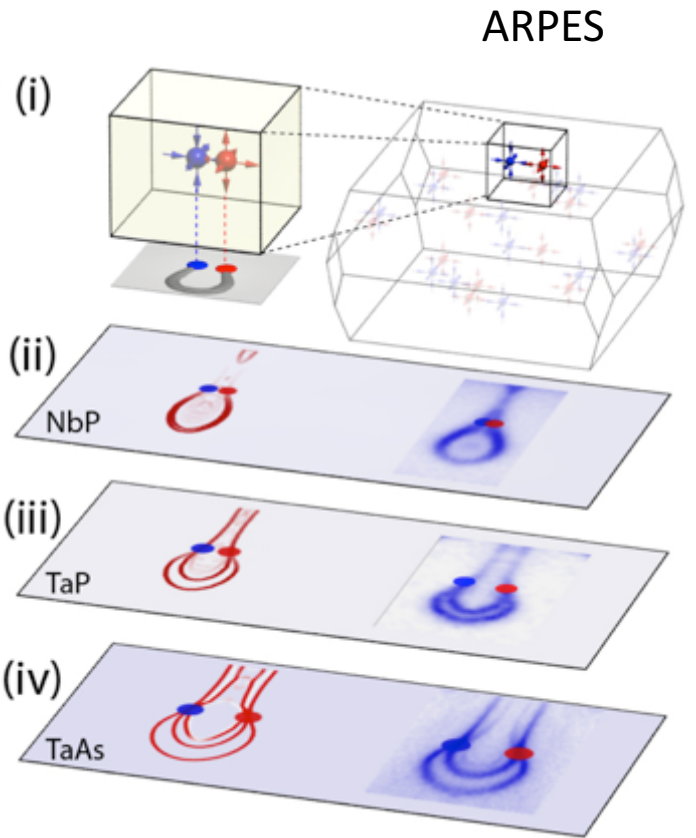
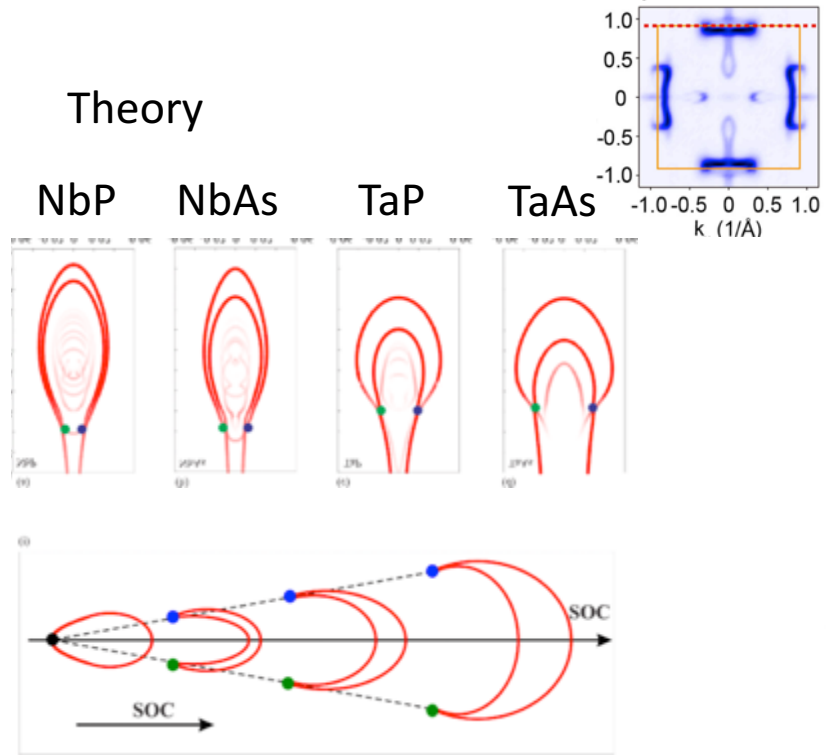
B. Q. Lv *et al.*, *Phys. Rev. X* **5**, 031013 (2015).  
 S.-Y. Xu *et al.*, *Science* **349**, 613 (2015).  
 L.X. Yang *et al.* *Nature Physics* **11**, 728 (2015).



Chemically boring!

1	2	3	4	5	6	7	8	9	10	11	12	13	14	15	16	17	18	19	20	21	22	23	24	25	26	27	28	29	30	31	32	33	34	35	36	37	38	39	40	41	42	43	44	45	46	47	48	49	50	51	52	53	54	55	56	57	58	59	60	61	62	63	64	65	66	67	68	69	70	71	72	73	74	75	76	77	78	79	80	81	82	83	84	85	86	87	88	89	90	91	92	93	94	95	96	97	98	99	100
H Hydrogen 1.00794	He Helium 4.002602											B Boron 10.811	C Carbon 12.0107	N Nitrogen 14.0067	O Oxygen 15.9994											Al Aluminum 26.9815	Si Silicon 28.0855	P Phosphorus 30.9738	S Sulfur 32.0650											As Arsenic 74.9216	Se Selenium 78.9600											Bi Bismuth 208.9804	Po Polonium (209)																																														
3	4	5	6	7	8	9	10	11	12	13	14	15	16	17	18	19	20	21	22	23	24	25	26	27	28	29	30	31	32	33	34	35	36	37	38	39	40	41	42	43	44	45	46	47	48	49	50	51	52	53	54	55	56	57	58	59	60	61	62	63	64	65	66	67	68	69	70	71	72	73	74	75	76	77	78	79	80	81	82	83	84	85	86	87	88	89	90	91	92	93	94	95	96	97	98	99	100		
Li Lithium 6.941	Be Beryllium 9.012182	Alkali Metal										Al Aluminum 26.9815	Si Silicon 28.0855	P Phosphorus 30.9738	S Sulfur 32.0650	Post-Transition Metal										As Arsenic 74.9216	Se Selenium 78.9600											Bi Bismuth 208.9804	Po Polonium (209)																																																												
19	20	21	22	23	24	25	26	27	28	29	30	31	32	33	34	35	36	37	38	39	40	41	42	43	44	45	46	47	48	49	50	51	52	53	54	55	56	57	58	59	60	61	62	63	64	65	66	67	68	69	70	71	72	73	74	75	76	77	78	79	80	81	82	83	84	85	86	87	88	89	90	91	92	93	94	95	96	97	98	99	100																		
K Potassium 39.0983	Ca Calcium 40.0780	Sc Scandium 44.9559	Ti Titanium 47.8670	V Vanadium 50.9415	Cr Chromium 51.9961	Mn Manganese 54.9380	Fe Iron 55.8450	Co Cobalt 58.9332	Ni Nickel 58.6934	Cu Copper 63.5460	Zn Zinc 65.3800	Ga Gallium 69.7230	Ge Germanium 72.6300	As Arsenic 74.9216	Se Selenium 78.9600											Bi Bismuth 208.9804	Po Polonium (209)																																																																								
37	38	39	40	41	42	43	44	45	46	47	48	49	50	51	52	53	54	55	56	57	58	59	60	61	62	63	64	65	66	67	68	69	70	71	72	73	74	75	76	77	78	79	80	81	82	83	84	85	86	87	88	89	90	91	92	93	94	95	96	97	98	99	100																																				
Rb Rubidium 85.4678	Sr Strontium 87.6200	Y Yttrium 88.9059	Zr Zirconium 91.2240	Nb Niobium 92.9064	Mo Molybdenum 95.9600	Tc Technetium (98)	Ru Ruthenium 101.0700	Rh Rhodium 102.9055	Pd Palladium 106.4200	Ag Silver 107.8682	Cd Cadmium 112.4110	In Indium 114.8180	Sn Tin 118.7100	Sb Antimony 121.7600	Te Tellurium 127.6000											Bi Bismuth 208.9804	Po Polonium (209)																																																																								
55	56	57	58	59	60	61	62	63	64	65	66	67	68	69	70	71	72	73	74	75	76	77	78	79	80	81	82	83	84	85	86	87	88	89	90	91	92	93	94	95	96	97	98	99	100																																																						
Cs Cesium 132.9054	Ba Barium 137.3270											Hf Hafnium 178.4900	Ta Tantalum 180.9479	W Tungsten 183.8400	Re Rhenium 186.2070	Os Osmium 190.2300	Ir Iridium 192.2170	Pt Platinum 195.0840	Au Gold 196.9666	Hg Mercury 200.5900	Tl Thallium 204.3833	Pb Lead 207.2	Bi Bismuth 208.9804	Po Polonium (209)											Bi Bismuth 208.9804	Po Polonium (209)																																																															

# A family photo of four compounds

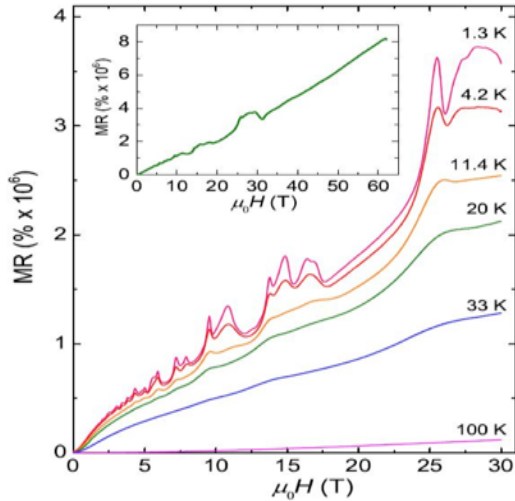


Y. Sun, S.-C. Wu, B. Yan, PRB 92, 115428 (2015)

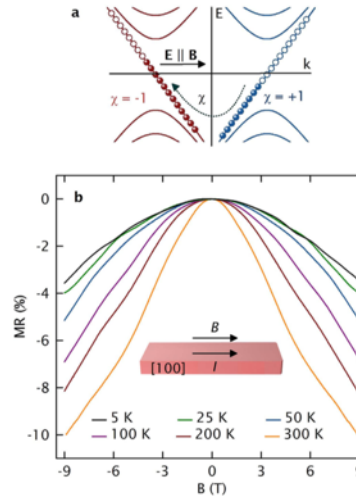
Z. K. Liu, et al Nature Mater.15,27 (2016)



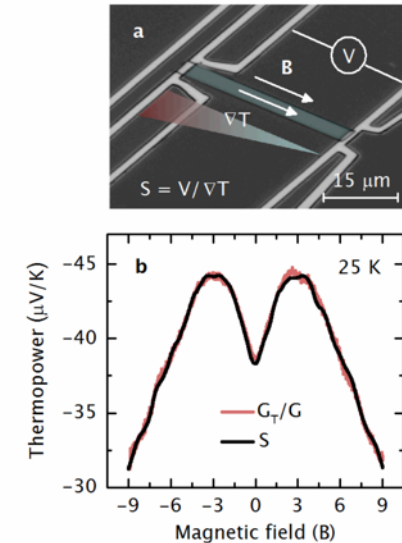
# Magneto-transport of WSMs



**Large MR and high mobility in NbP**



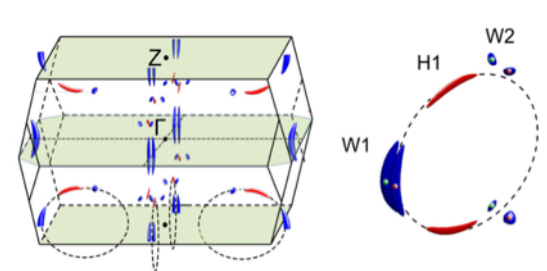
**Chiral anomaly,  
Negative LMR in TaP, NbP**



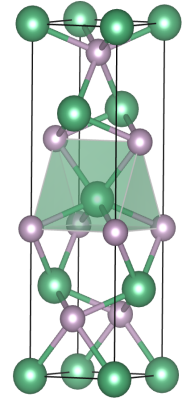
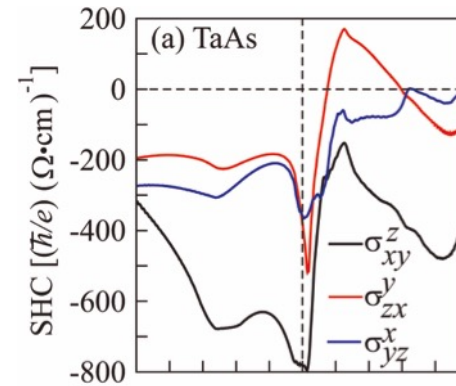
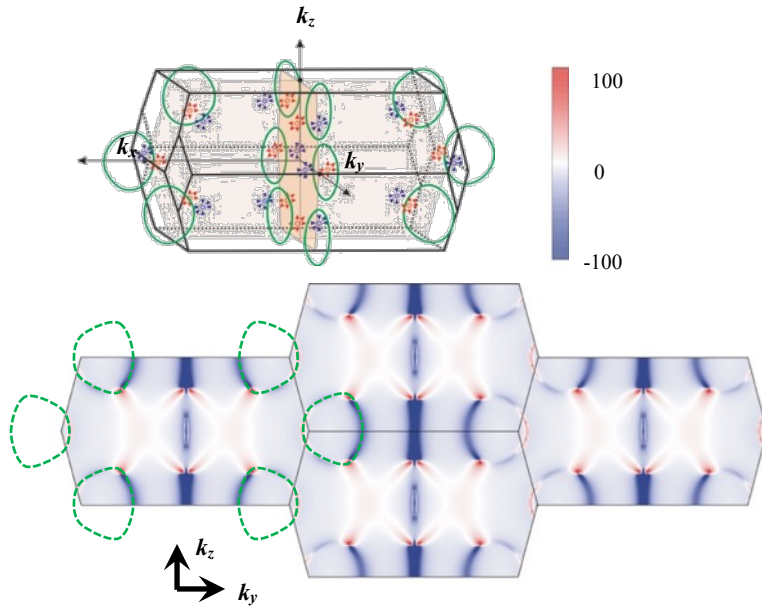
**Axial-gravitational anomaly  
in NbP**

(MPI Dresden)

- Shekhar et al. Nature Physics 11, 645 (2015)
- Arnold, F et al, Nature Comm. 7, 11615 (2016).
- Arnold, F et al, PRL 117, 146401, (2016).
- Niemann, A. C. et al. Sci. Rep. 7, 43394 (2017).
- Gooth J. et al. Nature 547, 324 (2017).



# Spin Hall Conductivity



$$\mathbf{J}_S \cdot \hat{y}^z = \sigma_{xy}^z \mathbf{J}_x$$

$$\sigma_{ij}^k = e\hbar \int_{BZ} \frac{d\vec{k}}{(2\pi)^3} \sum_n f_{n\vec{k}} \Omega_{n,ij}^k(\vec{k}),$$

$$\Omega_{n,ij}^k(\vec{k}) = -2Im \sum_{n' \neq n} \frac{\langle n\vec{k} | \hat{J}_i^k | n'\vec{k} \rangle \langle n'\vec{k} | \hat{v}_j | n\vec{k} \rangle}{(E_{n\vec{k}} - E_{n'\vec{k}})^2}$$

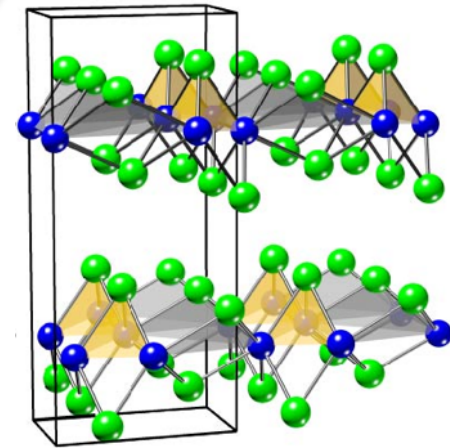
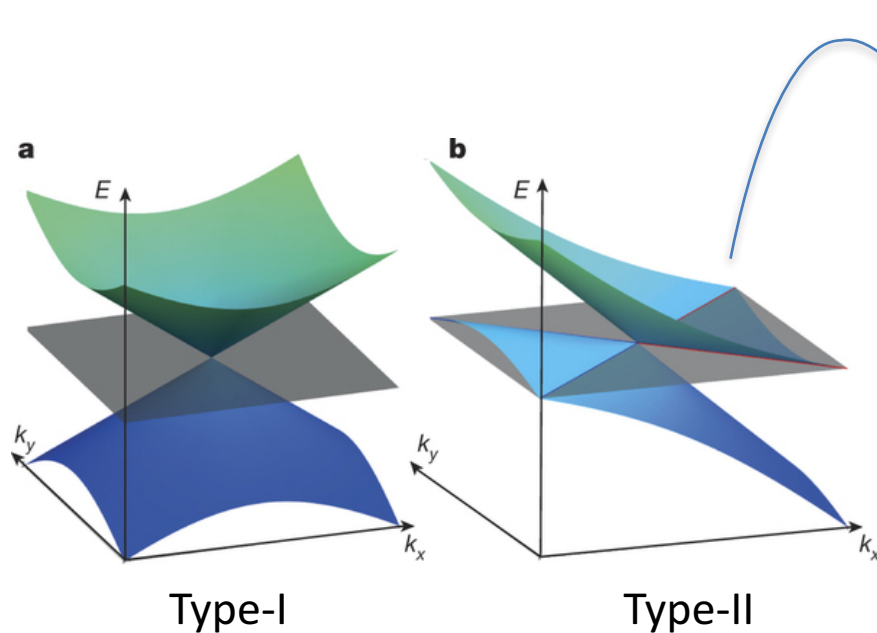
**Anisotropic**

$\sigma_{xy}^z \sim 800$  (TaAs)  
 $\sim 2000$  (Pt)

**Spin Hall Angle**

$\sigma^{\text{Spin}} / \sigma^{\text{charge}}$

# Two types of Weyl points



$\text{WTe}_2$ ,  $\text{MoTe}_2$

(Td phase with inversion breaking)

Stacking 2D TI layers into a WSM

A. A. Soluyanov et al. Nature **527**, 495 (2015). ( $\text{WTe}_2$ )

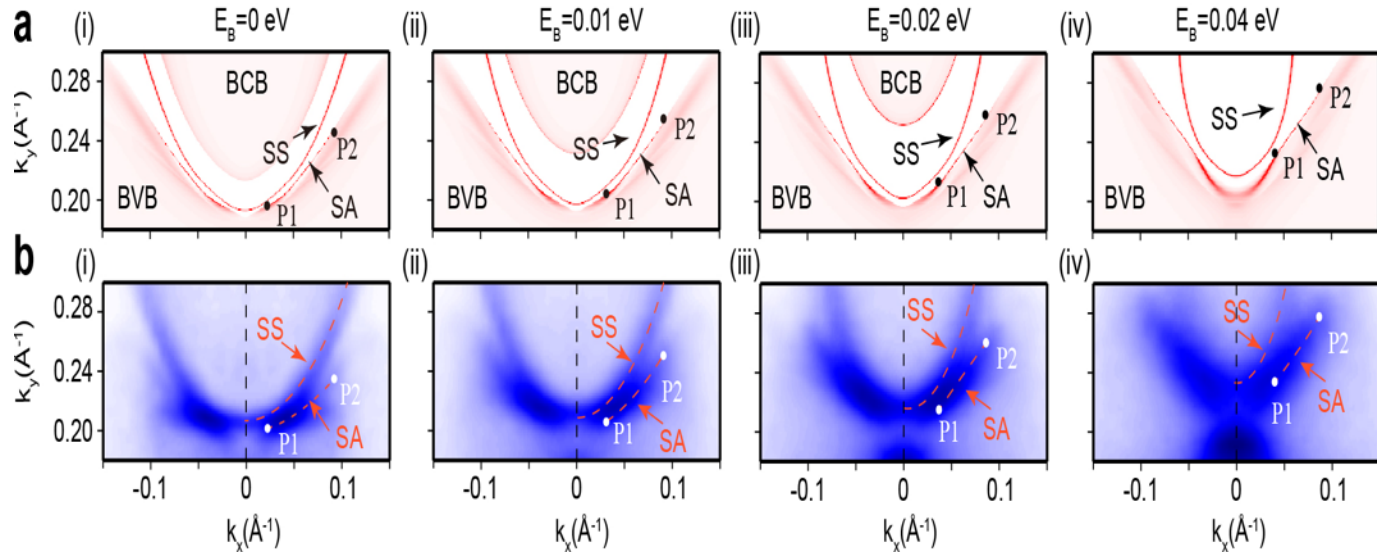
-  $\text{MoTe}_2$  -

Y. Sun, S.-C. Wu, M. N. Ali, C. Felser, and B. Yan, PRB **92**, 161107 (2015).

# MoTe<sub>2</sub> ARPES

Fermi surface

Theory

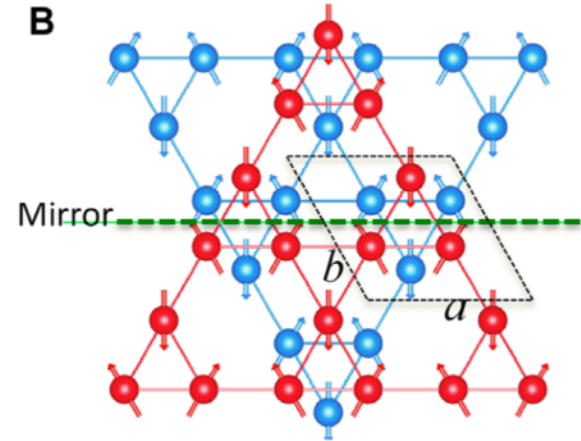
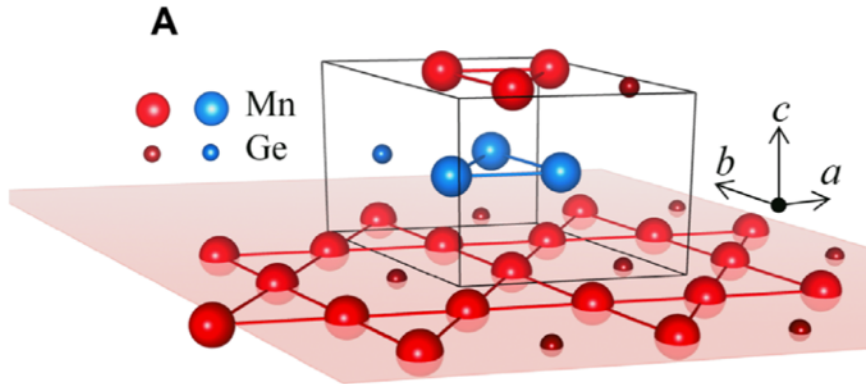


## ARPES:

- Deng, K. et al. *Experimental observation of topological Fermi arcs in type-II Weyl semimetal MoTe<sub>2</sub>*. Nature Physics 12, 1105–1110 (2016).
- Huang, L. et al. *Spectroscopic evidence for a type II Weyl semimetallic state in MoTe<sub>2</sub>*. Nature Materials 15, 1155–1160 (2016).
- Jiang, J. et al. **Signature of type-II Weyl semimetal phase in MoTe<sub>2</sub>**. Nature Commun. 8, 13973 (2017).
- Tamai, A. et al. *Fermi Arcs and Their Topological Character in the Candidate Type-II Weyl Semimetal MoTe<sub>2</sub>*. Phys. Rev. X 6, 031021 (2016).
- Liang, A. et al. *Electronic Evidence for Type II Weyl Semimetal State in MoTe<sub>2</sub>*. arXiv:1604.01706 (2016).
- Sakano, M. et al. *Observation of spin-polarized bands and domain-dependent Fermi arcs in polar Weyl semimetal MoTe<sub>2</sub>*. Phys. Rev. B 95, 121101 (2017).

# AFM WSMs from AHE materials

**Room-temperature** non-collinear AFM in the Kagome lattice

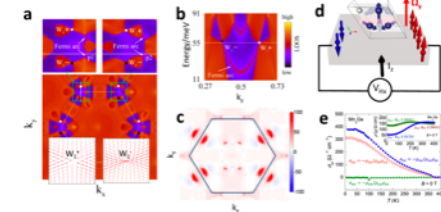
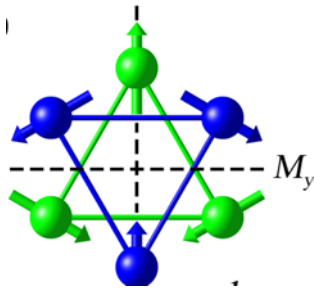


Observation of strong **AHE**:  
Mn<sub>3</sub>Sn (Tokyo) Nature 527, 212 (2015)  
Mn<sub>3</sub>Ge (MPI) Sci. Adv. 2, e1501870 (2016)

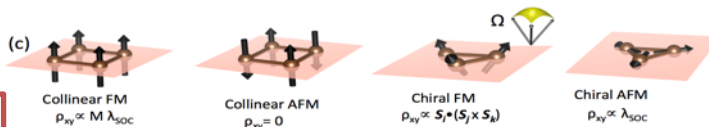
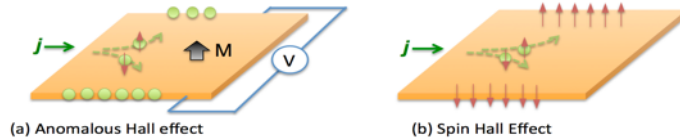
Observation of strong **SHE**  
Mn<sub>3</sub>Ir (MPI) Sci. Adv. 2, e1600759 (2016)

All spins align in-plane.

# AFM Weyl, AHE and SHE



- Mn<sub>3</sub>Sn • AFM WSMs
- Mn<sub>3</sub>Ge • Anomalous Hall and Nernst effects (AHE & ANE) at room temperature
- Intrinsic spin Hall effect due to spin texture (without SOC)



AHE

SHE

$\lambda_{SOC}$

$\lambda_{SOC}$

$\lambda_{SOC} ?$

$\lambda_{SOC} ?$

TRS

0

$\lambda_{SOC}$

Nayak, A. K. *et al. Science Advances* **2**, e1501870–e1501870 (2016).  
 Zhang, W. *et al. Science Advances* **2**, e1600759–e1600759 (2016).  
 Yang, H. *et al. New Journal of Physics* **19**, 015008 (2017).  
 Zhang, Y. *et al. Physical Review B* **95**, 075128 (2017).

Železný, J., Zhang, Y., Felser, C. & Yan, B. arXiv:1702.00295  
 Šmejkal, L., Mokrousov, Y., Yan, B. & MacDonald, A. H. arXiv:1706.00670

# Weyl materials

Linear response to a *dc* electric field field

## **SHE & AHE**

- Both Weyl and ordinary bands contribute to AHC.
- Conventional materials work well.

***Are there some properties for which a WSM is unique or better than ordinary materials?***

Yes, possibly the nonlinear optical response.

# Nonlinear optical response

Second-order nonlinear response to the oscillating E-field of light

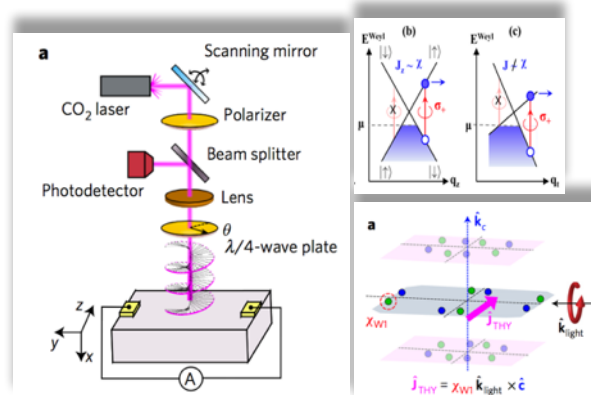
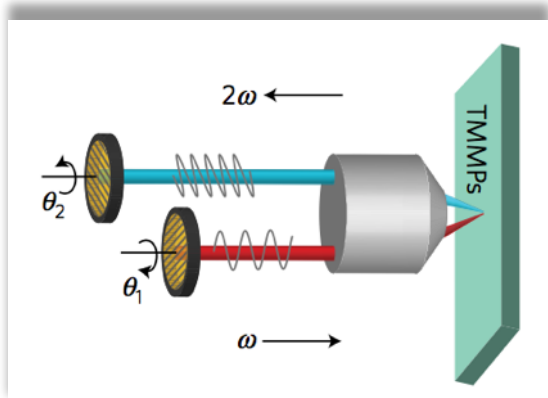
- Circular photogalvanic effect (CPGE)
- Second harmonic generation (SHE)

$$E_c(t) = \text{Re}\{\mathcal{E}_c e^{i\omega t}\}$$

$$j_a = \text{Re}\{j_a^0 + j_a^{2\omega} e^{2i\omega t}\}$$

$$j_a^{(2\omega)} = \chi_{abc} \mathcal{E}_b \mathcal{E}_c$$

$$j_a^{(0)} = \chi_{abc} \mathcal{E}_b \mathcal{E}_c^*$$

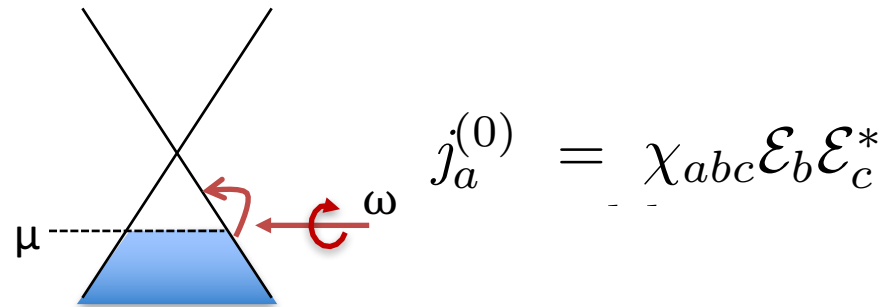
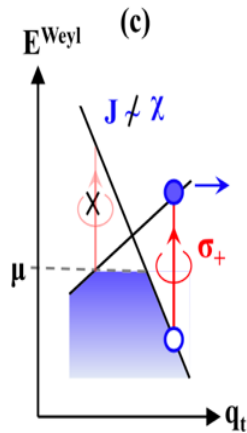
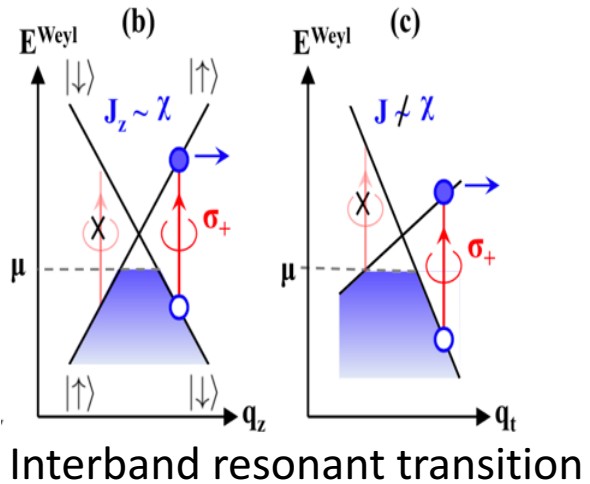


**Experiment** on WSM TaAs: Orenstein 17', Gedik 17', Wang 17'

**Theory:** Qi 15', Pesin 15', Burkov 15', Ran 16', Fu 15', Moore 16' 17', Polini 17', Nagaosa 16', Tanaka 16', Lee 17'...



# Nonlinear optical response



$$j_a^{(0)} = \chi_{abc} \mathcal{E}_b \mathcal{E}_c^*$$

Intraband transition (low frequency)

$$j_a = j_a^{(2\omega)} |_{\omega \rightarrow 0} = 2\chi_{abb} |\mathcal{E}_b|^2$$

At dc limit comes a nonlinear Hall effect.

[1] J. E. Moore and J. Orenstein, Phys. Rev. Lett. **105**, 026805 (2010).

[2] E. Deyo, L. E. Golub, E. L. Ivchenko, and B. Spivak, (2009), arxiv:0904.1917.

[3] I. Sodemann and L. Fu, Phys. Rev. Lett. **115**, 216806 (2015).

# Semiclassical theory

Current

$$j_a = -e \int_k f(k) v_a$$

Anomalous velocity

$$v_a = \partial_a \epsilon(k) + \epsilon_{abc} \Omega_b \dot{k}_c,$$

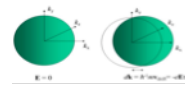
Light field

$$\dot{k}_c = -e E_c(t), \quad E_c(t) = \text{Re}\{\mathcal{E}_c e^{i\omega t}\}$$

Solve the Boltzmann equation to the second order  $-e\tau E_a \partial_a f + \tau \partial_t f = f_0 - f$

$$j_a = \text{Re}\{j_a^0 + j_a^{2\omega} e^{2i\omega t}\} \quad j_a^{(0)} = \chi_{abc} \mathcal{E}_b \mathcal{E}_c^* \quad j_a^{(2\omega)} = \chi_{abc} \mathcal{E}_b \mathcal{E}_c$$

$$\chi_{abc} = \epsilon_{adc} \frac{e^3 \tau}{2(1 + i\omega\tau)} \int_k (\partial_b f_0) \Omega_d$$



TRS

$$\Omega_c(k) = -\Omega_c(-k)$$

$$\sigma_{ab} = -\epsilon_{abc} \frac{e^2}{\hbar} \int_k f_0 \Omega_c = 0$$

$$\int_k f_0 \Omega_c = 0$$

$$\int_k (f_0 + \partial_k f_0) \Omega_c = \int_k \partial_k f_0 \Omega_c \neq 0$$

[1] J. E. Moore and J. Orenstein, Phys. Rev. Lett. **105**, 026805 (2010).

[2] E. Deyo, L. E. Golub, E. L. Ivchenko, and B. Spivak, (2009), arxiv:0904.1917.

[3] I. Sodemann and L. Fu, Phys. Rev. Lett. **115**, 216806 (2015).

# Semiclassical theory

Current

$$j_a = -e \int_k f(k) v_a$$

Anomalous velocity

$$v_a = \partial_a \epsilon(k) + \epsilon_{abc} \Omega_b \dot{k}_c,$$

Light field

$$\dot{k}_c = -e E_c(t), \quad E_c(t) = \text{Re}\{\mathcal{E}_c e^{i\omega t}\}$$

Solve the Boltzmann equation to the second order  $-e\tau E_a \partial_a f + \tau \partial_t f = f_0 - f$

$$j_a = \text{Re}\{j_a^0 + j_a^{2\omega} e^{2i\omega t}\} \quad j_a^{(0)} = \chi_{abc} \mathcal{E}_b \mathcal{E}_c^* \quad j_a^{(2\omega)} = \chi_{abc} \mathcal{E}_b \mathcal{E}_c$$

$$\chi_{abc} = \epsilon_{adc} \frac{e^3 \tau}{2(1 + i\omega\tau)} \int_k (\partial_b f_0) \Omega_d = -\epsilon_{adc} \frac{e^3 \tau}{2(1 + i\omega\tau)} \int_k \underline{f_0(\partial_b \Omega_d)}$$

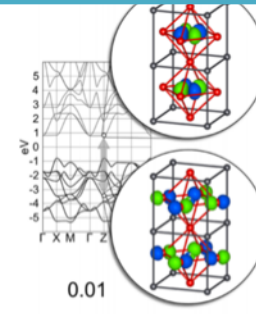
Berry curvature dipole

$$D_{ab} = \int_k f_0(\partial_a \Omega_b).$$

- Intrinsic to the band structure
- Inversion symmetry breaking
- A Fermi surface property

# *Ab initio* calculations

Interband transitions are extensively studied for insulators, e.g. Rappe 12', Sipe and Shkrebtii 00'



## Current work on intraband contributions in the Berry curvature dipole formalism

1. DFT (GGA) band structure and Bloch wave functions  
two representative families: Type-I TaAs, type-II MoTe<sub>2</sub>
2. *Highly symmetric* Wannier functions for a single-particle Hamiltonian
3. Berry curvature  $\Omega$

$$\Omega_a^n(\mathbf{k}) = 2i \sum_{m \neq n} \frac{\langle n | \partial_{k_b} \hat{H} | m \rangle \langle m | \partial_{k_c} \hat{H} | n \rangle}{(\epsilon_n - \epsilon_m)^2} \quad \text{Xiao 10'}$$

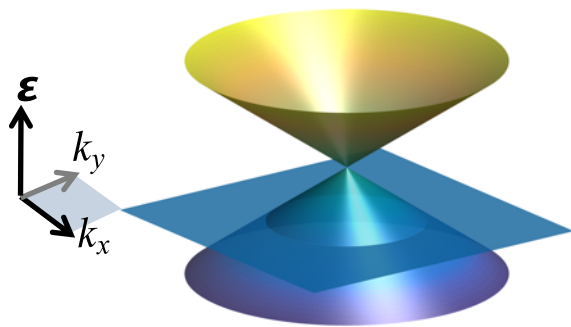
4. Berry curvature dipole  $\mathbf{D}$ , a tensor  $D_{bd} = \int_{\mathbf{k}} f_0 \frac{\partial \Omega_d}{\partial k_b}$  Fu 15'

# Start with toy models

A single Weyl cone

$$H_{Weyl}(\mathbf{q}) = \hbar v_t q_t \sigma_0 + \hbar v_F \mathbf{q} \cdot \boldsymbol{\sigma},$$

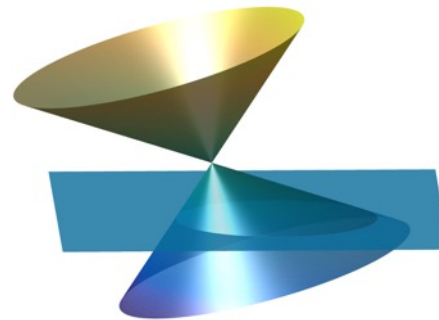
(a) Type-I



Berry curvature

$$\Omega(\mathbf{q}) = \frac{\mathbf{q}}{2q^3}$$

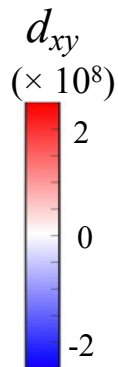
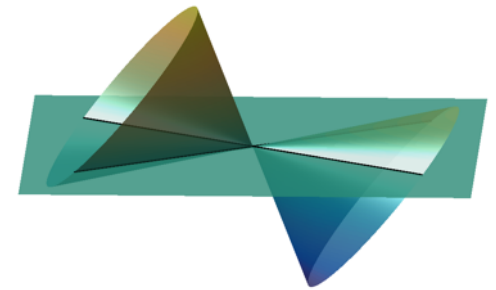
(b) Type-I (titled)



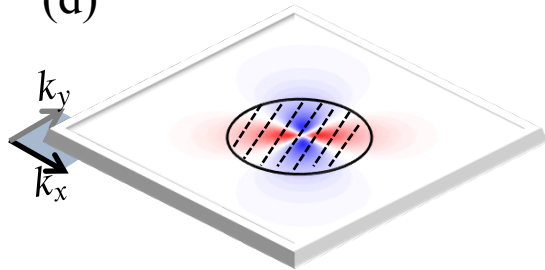
Berry curvature dipole

$$d_{xy} = \frac{\partial \Omega_y}{\partial q_x} = \frac{3q_x q_y}{2q^5}$$

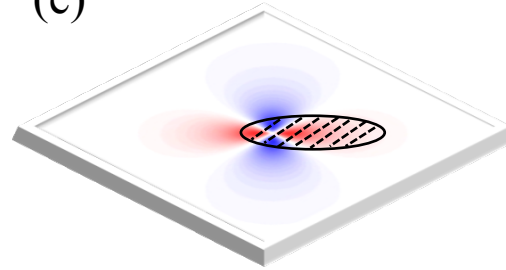
(c) Type-II



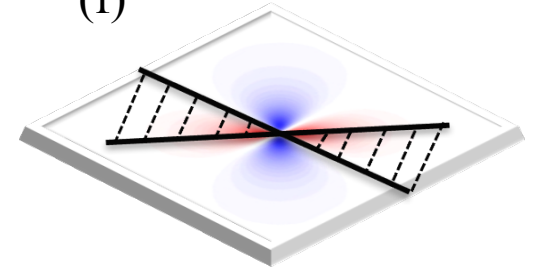
(d)



(e)



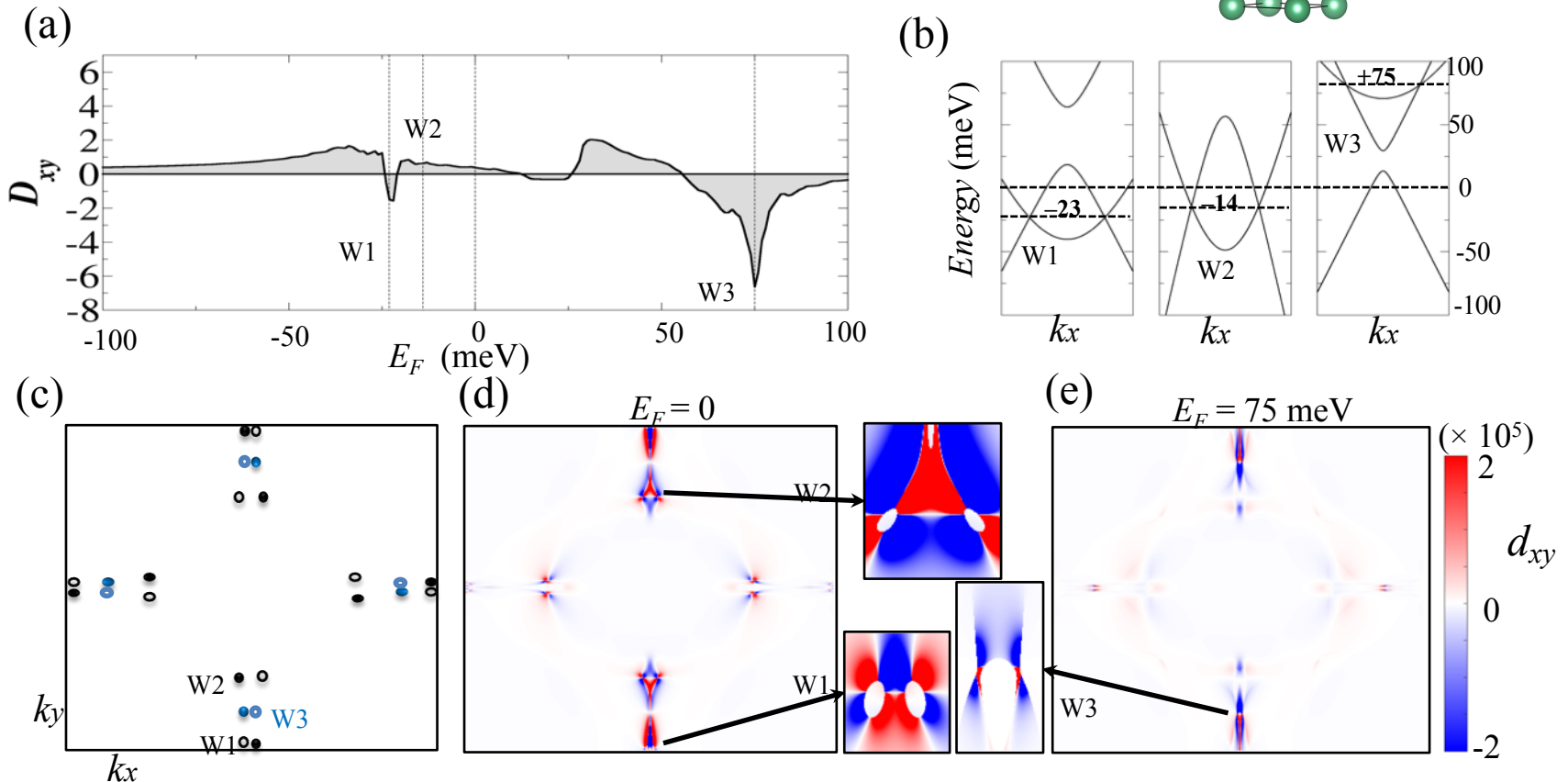
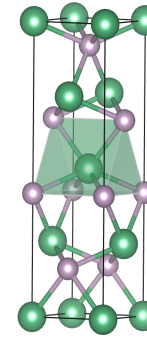
(f)



Note that  $d_{xy} = \partial \Omega_y / \partial k_x$  is **even** to  $M_x$ ,  $M_y$  or  $TRS$ .  
So a pair of Weyl points contribute the same  $D_{xy}$ .

# Berry curvature dipole for TaAs

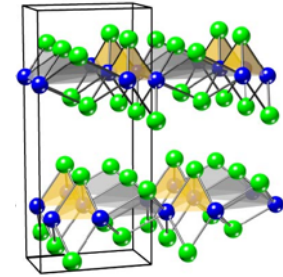
- Point group  $C_{4v}$ :  $M_x, M_y, C_4$   
*E.g.  $M_x$ :  $k_x \rightarrow -k_x, \Omega_x \rightarrow \Omega_x$  so  $d_{xx} \rightarrow -d_{xx}$  then  $D_{xx} = 0$*   
*Finally we have **only one** independent element  $D_{xy} = -D_{yx}$*



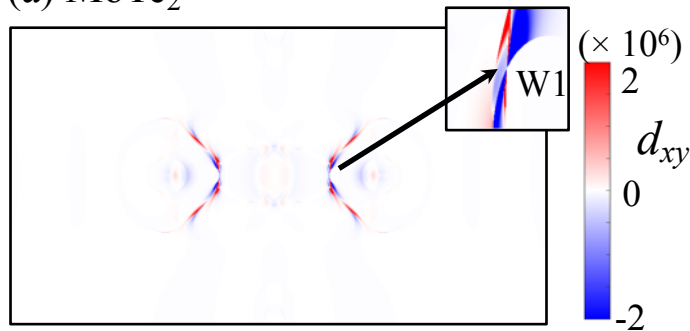
# Berry curvature dipole for $\text{MoTe}_2$ and $\text{WTe}_2$

- Point group  $C_{2v}$

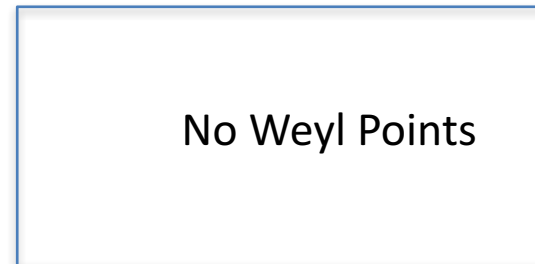
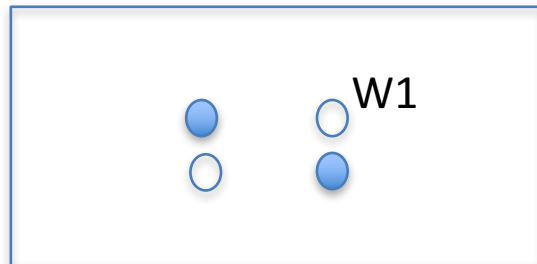
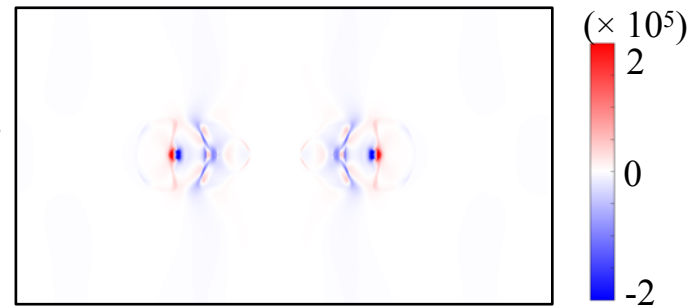
Finally we have two independent element  $D_{xy}$  and  $D_{yx}$



(a)  $\text{MoTe}_2$



(b)  $\text{WTe}_2$



# Berry curvature dipole

Material	$D_{xy}$	Material	$D_{xy}$	$D_{yx}$
TaAs	0.39	MoTe <sub>2</sub>	0.849	-0.703
TaP	0.029	WTe <sub>2</sub>	0.048	-0.066
NbAs	-9.88			
NbP	20.06			

- WSM is better than non-WSM
- Type-II is generally better than type-I
- $D_{xy}$  is not scaled by SOC, different from SHE
- A pair of Weyl points related by  $M_{x,y}$  or TRS contribute the same  $D_{xy}$



# Estimation for the nonlinear Hall effect

Material	$D_{xy}$	Material	$D_{xy}$	$D_{yx}$
TaAs	0.39	MoTe <sub>2</sub>	0.849	-0.703
TaP	0.029	WTe <sub>2</sub>	0.048	-0.066
NbAs	-9.88			
NbP	20.06			

$$\chi_{abc} = -\varepsilon_{adc} \frac{e^3 \tau}{2\hbar^2 (1 + i\omega\tau)} D_{bd}$$

$D_{xy}$  corresponds to  $\chi_{zxx}$  and  $\chi_{xxz}$

$d_{xy} = \partial\Omega_y / \partial k_x$   
*x*: the current direction  
*y*: berry curvature (B field)  
*z*: Hall current

$$j_z = 2\chi_{zxx} \mathcal{E}_x^2 \quad j_x = \sigma_{xx} \mathcal{E}_x$$

a Hall angle as  $\gamma = j_z / j_x = 2(\chi_{zxx} / \sigma_{xx}) \mathcal{E}_x$

AHE systems  $\gamma \sim 10^{-3}$

$$\tau \sim 10 \text{ ps and } \sigma_{xx} \sim 10^6 \Omega^{-1} \text{m}^{-1}$$

$$\mathcal{E}_x \sim 10^2 \text{ V/m}$$

$$\chi_{zxx} \sim 10^{-1} D_{xy}$$

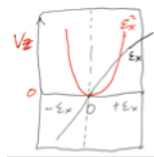
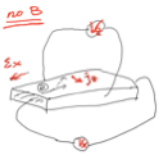
$$\gamma \sim 10^{-5} - 10^{-4}$$

For TaAs, NbPAs, NbP, MoTe<sub>2</sub>

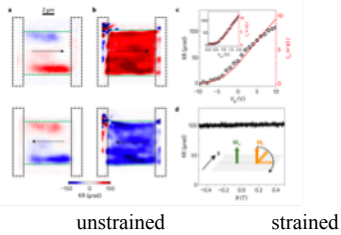
# Estimation for the nonlinear Hall effect

Material	$D_{xy}$	Material	$D_{xy}$	$D_{yx}$
TaAs	0.39	MoTe <sub>2</sub>	0.849	-0.703
TaP	0.029	WTe <sub>2</sub>	0.048	-0.066
NbAs	-9.88			
NbP	20.06			

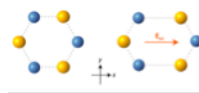
$$j_z = 2\chi_{zxx}\mathcal{E}_x^2 \quad j_x = \sigma_{xx}\mathcal{E}_x$$



# Signatures in earlier experiments

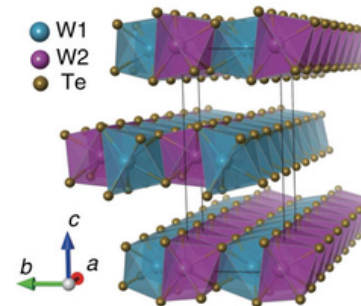


Valley magnetoelectricity in single-layer MoS2



Lee, J., Wang, Z., Xie, H., Mak, K. F. & Shan,  
*Nature Materials* **16**, 887–891 (2017).

Kerr rotation image of a single-layer MoS2 device

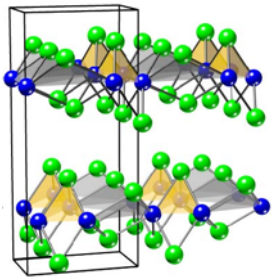
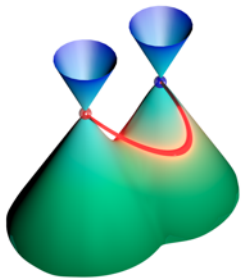


WTe2 ?  
Inversion breaking  
Weyl, QSH  
Superconductor

NMR, Spin current

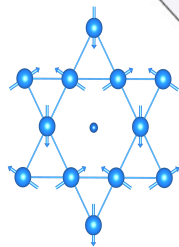
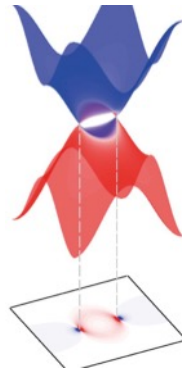
# Summary

Topological materials



- Topological materials
- Experiments

Berry curvature  
Linear response

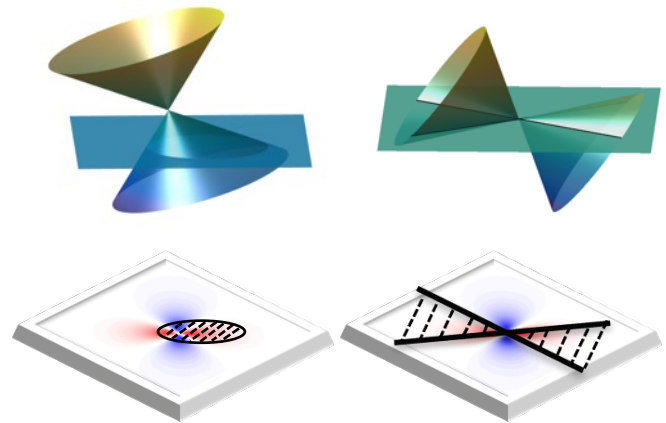


Mn<sub>3</sub>Ge and Mn<sub>3</sub>Sn

AFM Weyl  
AHE, ANE  
SHE w/o SOC

- Berry phase induced electric and optical properties
- Develop ab initio tools

Berry curvature dipole  
Nonlinear response



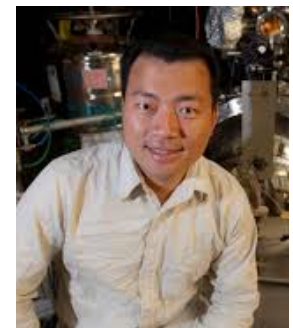
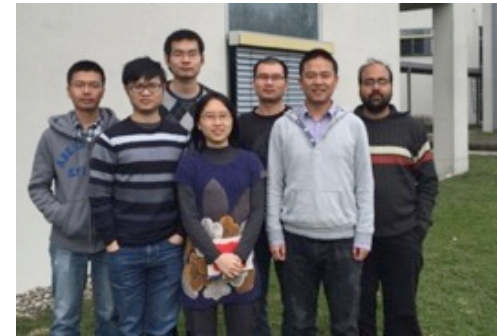
# Acknowledgement

Collaborators  
(MPI Dresden):

- Claudia Felser
- **Yan Sun , Yang Zhang, Yang Hao**
- Ady Stern (Weizmann)
- Haim Beidenkopf (Weizmann)
- Yu-Lin Chen (Oxford)
- Liang Fu (MIT)
- Kin Fai Mak (Penn State U)
- Di Xiao (Carnegie Mellon U)
- Stuart Parkin (MPI Halle)



MAX-PLANCK-GESELLSCHAFT



Thanks for your attention!

